ISSN (Print) 1226-1750
ISSN (Online) 2233-6656
Journal of Magnetics 25(4), 632-638 (2020) https://doi.org/10.4283/JMAG.2020.25.4.632

Deeplab v3+ Based Automatic Diagnosis Model for Dental X-ray: Preliminary Study

Young-Jin Jung[1]* and Min-Ji Kim[2]

[1]*Department of Radiological Science, Dongseo University, Busan, Republic of Korea*
[2]*Department of Dental Hygiene, Dongseo University, Busan, Republic of Korea*

(Received 1 November 2020, Received in final form 10 December 2020, Accepted 10 December 2020)

Recently, deep learning (DL) based semantic segmentation approach has been widely applied in medical image analysis. The semantic segmentation approach based DL technique was employed in the diagnosis of dental conditions with digital panoramic radiography (DRP). The purpose of this study is to investigate the accuracy of the semantic segmentation of Deeplab v3+ in the diagnosis of 5 different dental disease - apical, abrasion, caries, impaction, perio. DPR database (512×748-pixel, including 86 panoramic radiography) was used for semantic segmentation (DeepLab v3+). To validate the performance, the confusion matrix (maximum 97 %) was estimated. In addition, significant classification and semantic segmentation results were assessed. From the result of this study, the DL model could be a useful tool for the dentist to identify dental diseases as a clinical aid software.

Keywords : artificial intelligence, computed-aided diagnosis, electromagnetic radiation image, dental radiography, ionizing radiation image

1. Introduction

During the last decade, Artificial intelligence (AI) is sharply widely researched as a clinical application in dentistry [1]. The various development, application, and performance of AI in dentistry was studied and demonstrated for clinical potential. Since 1955, AI has been widely recognized by John McCarthy who coined the term AI [2].

In 1984, John said that "for any AI that we might build which had mental states equivalent to human mental states, the implementation of a computer program would not by itself be sufficient. Rather the artifact intelligence would have to have powers equivalent to the powers of the human brain" [3]. In other words, AI can show abilities, which including learning, problem-solving, and decision making associated with human's thinking

There were various terms for AI was used for automated clinical application such as AI, Machine Learning, Neural Networks, and Deep Learning. The term AI refers to everything that a computer or machine behaves or thinks and judges like a human being. The term machine learning (ML) is a part of AI. Machine Learning means a learning technique for machines or computers like humans to solve certain problems through specific learning techniques based on the dataset. Finally, Neural Network or Deep Learning is one of the techniques of machine learning, and it refers to a mathematical algorithm that mimics the human thinking process based on neuron activities. where, if the number of hidden layers is one or a few, it is called Neural Networks, and those that reach tens to hundreds of layers are called Deep Learning.

Over the past few years, AI that can automatically guide to identify the human disease was sharply developed as an edge medical technology. Especially, the A.I. technology demonstrated tremendous potential using radiographic images (such as X-ray, Computed Tomography, Magnetic Resonance Imaging, Positron Emission Tomography, etc). Especially, Watson is the first AI technology that was utilized to diagnose and treatment for human cancer. In 2016, 'Watson For On Cology' was set up at Gil Hospital, Gachon University in Incheon (Weekly sympathy, Jan. 26. 2017) [4], 'Watson for Genomics' which recommends treatment through analysis using cancer cell and gene sequence, was installed in Pusan National University Hospital (Kukje Newspaper,

*Corresponding author: Tel: +82-51-320-2871
Fax: +82-51-320-2732 , e-mail: microbme@outlook.com

Jan. 24. 2017) [5]. In addition, 7 hospitals including Keimyung University Dongsan Hospital, Daegu Catholic University Hospital, Konyang University Hospital, Chosun University Hospital, and Chonnam National University Hospital employed Watson. Although, the Ministry of Food and Drug Safety classified Watson as a 'non-medical device' by announcing the 'Guidelines for the approval and examination of medical devices with big data and artificial intelligence technology'. (Health Chosun, Jan. 11. 2018) [6]. There is still a high potential for diagnostic success demonstrated by AI.

In particular, the current AI technology has shown sufficient performance in analyzing simple images only under specific conditions in Human tissue [1]. One of the areas with high potential in dentistry. In the case of dental X-ray images, the imaging conditions are very constant, and the shape of the human tissue being photographed is very similar. Also, it is very likely to show a high diagnostic success rate through the application of the AI based computational technology since the types of diseases that can be identified through photographs are limited.

Recently, AI has been used in dentistry as an important tool to build an automated guiding process of diagnosis for more accuracy and efficiency. The AI is currently recognized as the most popular medical aid technology, and accordingly, various studies are being actively conducted in the world [1, 7-11]. In particular, Casalegno (2019) demonstrated that near-infrared transillumination imaging is effective for the detection of early-stage lesions (5 types) using AI [12]. Ekert (2019) showed that the deep convolution neural networks (CNN) on a limited amount of image data showed satisfying discriminatory ability to detect apical lesions on panoramic radiographs [13]. Hung (2019) insisted that clinicians are encouraged to adopt the AI algorithms for early intervention and treatment of root caries for the aging population from his study (prediction of root caries using Machine Learning) [14]. Schwendicke (2020) studied to detect the caries lesion using deep learning with near-infrared light transillumination images. From this study, the deep CNN trained on a limited amount of NILT image data demonstrated successive discriminatory ability to detect caries lesions [15].

Since imaging tests are essential for pre-treatment disease state evaluation, and post-treatment response evaluation, the proportion of readings in imaging tests is increasing, and it is highly likely to show a high diagnostic success rate through the application of AI technology [16]. However, the number of teeth handled in the dental field is larger (28 teeth) than other departments, and due to the oral environment in which sensory nerves are intensively developed, there are many items to be considered when evaluating the prognosis of the disease [17]. For classification, each tooth was classified by applying a ResNet-based (backbone) Mask R-CNN using 846 panoramic images. Wisdom teeth were detected using 838 panoramic images, and numbers were marked on the classified teeth using 1,352 panoramic images [18].

The aim of the current AI study using X-ray radiograph was to classify the different five lesions (perio, caries, apical, impaction, abrasion) and sound using deep learning. The Deeplab_v3 based AI model was employed to

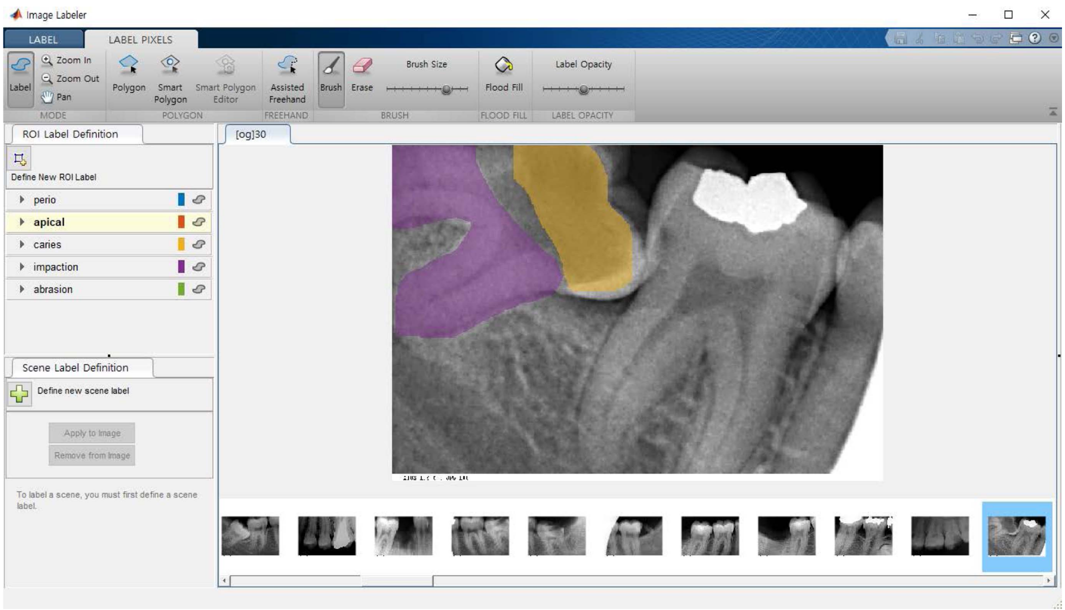

Fig. 1. (Color online) Manual ground truth labeling using the image labeler in MATLAB.

analyze the X-ray radiograph and to evaluate the classification performance and its features of the lesion area.

2. Materials and Methods

2.1. Data-set

This study used 512×748-pixel of 120 periapical views of apical, perio, abrasion, impaction, caries, and sound, respectively which were collected from Kaggle (www.kaggle.com, Machine Learning, and data science community). The present retrospective study was approved by the institutional review board of Dongseo University in accordance with proper ethics procedures (2020-020-HR-01).

2.2. Ground truth labeling

MATLAB2020a software (MathWorks Inc., Natick, MA, USA) was used for the pixel-based ground-truth labeling. The pixel-based ground truth labeling was manually conducted using the Image Labeler tool (included in MATLAB2020b) by Oral and Maxillofacial Radiology professional specialists between March 2020 and October 2020 (Fig. 1). 6 different categories were labeled; apical, abrasion, caries, impaction, perio, sound. Among the categories, 5 categories (apical, abrasion, caries, impaction, perio) were manually labeled and exported as ground truth files. The sound category was labeled using live scripting on the ground truth files; all array contains 0 (no label) values were declared as 'sounds'.

2.3. DeepLab_v3+

To train and test the pixel-labeled database, the DeepLab-v3+ was employed. MATLAB2020b software was used to run the DeepLab-v3+. It comprised of 100 layers for convolution neural network process, that generally used for semantic image segmentation as a deep learning approach. The neural network model designed based on the well-known ResNet18. The DeepLab-v3+ is designed with the encoder/decoder structure (Fig. 2). This specific structure is suitable for the semantic segmentation process. The encoder module is designed to extract the image features similar to the forward propagation process of the classification problems. This module is also considered to reduce the size of the data by down-sampling approach; pooling layers. This down-sampled data reduces the GPU memory loss during the calculation, propagating the high-level activation to the next layers. Also, the encoding module includes an atrous convolution approach (Fig. 3). This specific convolution method has strided convolution kernel as shown in Fig. 2-1. This "holed" kernel is considered to have high activation for a larger object in the same calculation burden of the general convolution kernel. Regarding that the semantic segmentation is a problem with large and glomerated objects,

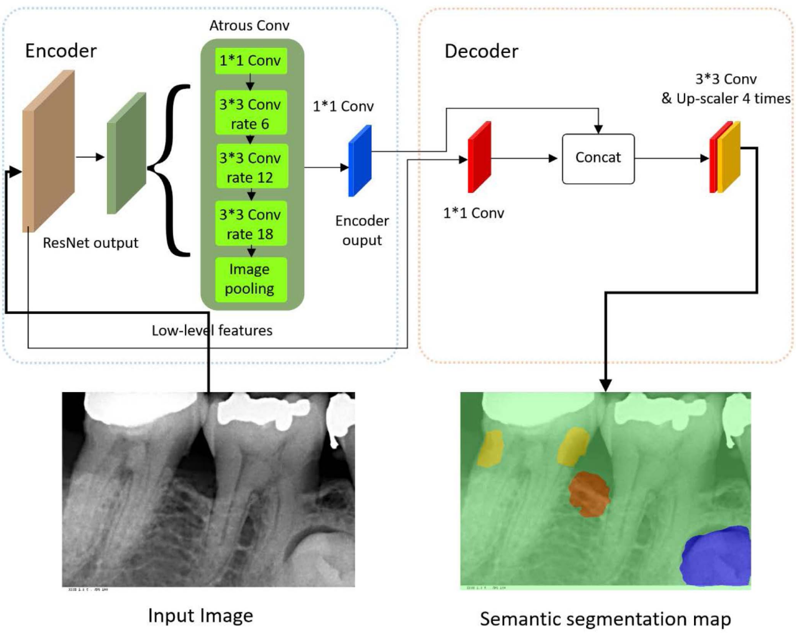

Fig. 2. (Color online) Convolutional Encoder-Decoder Architecture. The left side image describes the ResNet model (Encoder) to estimate the dental diseases using the "input image" (dental radiography). The right side image depicts the Decoder to reconstruct the semantic segmentation image from the dental disease feature.

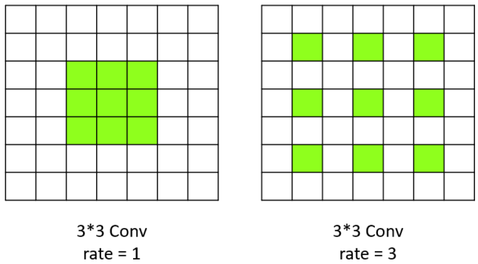

Fig. 3. (Color online) Atrous convolution kernel. The left image is the 3 × 3 kernel when ‘rate’ is 1. The right side image is the other 3 × 3 kernel when ‘rate’ is 3.

the atrous convolution approach is considered to avoid the activation of the small features. The decoder module is an upsampling process to enlarge the output of the encoder module, which has a smaller data size and samples than the original input data.

2.4. Training Progress

For the training progress, 2 kinds of model validation were conducted for training and testing; the Model-1 – whole 86 images were trained and the model was tested with the same 86 images (epoch = 10, learning rate = 0.01), the Model-2 - the ratio of training/test data was set 7:3. All experiments were conducted with a general PC with Nvidia GeForce RTX 2070 GPUs, 32.0GB RAM, AMD Ryzen 7 3800X 8-Core Processor (3893 Mhz, 8 core, 16 logic processor).

2.5. Confusion Matrix

The confusion matrix (CM) is a table that is widely used to describe the performance of an AI classification model (as a “classifier”). It was conducted on a set of test data for which the true values are know based on pixel calculation. The confusion matrix can be comprised of two class groups: “Actual class group” and “Predicted class group”. In this study, we have 6 classes: apical, abrasion, caries, impaction, perio, sound (normal area). To validate the performance of the selected AI model for X-ray radiography in dentary, two kinds of validation results were calculated. Two matrix (model-1 is 6 by 6 by 86, and model-2 is 6 by 6 by 26) was calculated. In order to get the final CM (fCM), two matrices were summed based on the three-dimensional axis (trial dimension: 86 &26). In addition, the accuracy matrix also calculated based on the fCM as follow:

$$\text{Accuracy} = \frac{\text{True Positive}}{\text{True Positive} + \text{True Nagatives}}$$

3. Results and Discussion

3.1. Training progress

Figure 4 and 5 show the overall training progress of both model 1 and model. In the training progress plot, a blue-colored line refers to the normalized training accuracy (%) and the orange-colored line refers to the loss of training. Model 1 showed an elapsed time of 110 sec for 10 epochs and resulted in 98.47 % mini-batch accuracy, keeping about 90% accuracy from the 1 st epoch (Fig. 4-1 and Table 1).

Model 2 showed the elapsed time of 97 sec for 10 epochs and resulted in 98.55 % of mini-batch accuracy, keeping about 90 % accuracy from the 1st epoch (Fig. 5

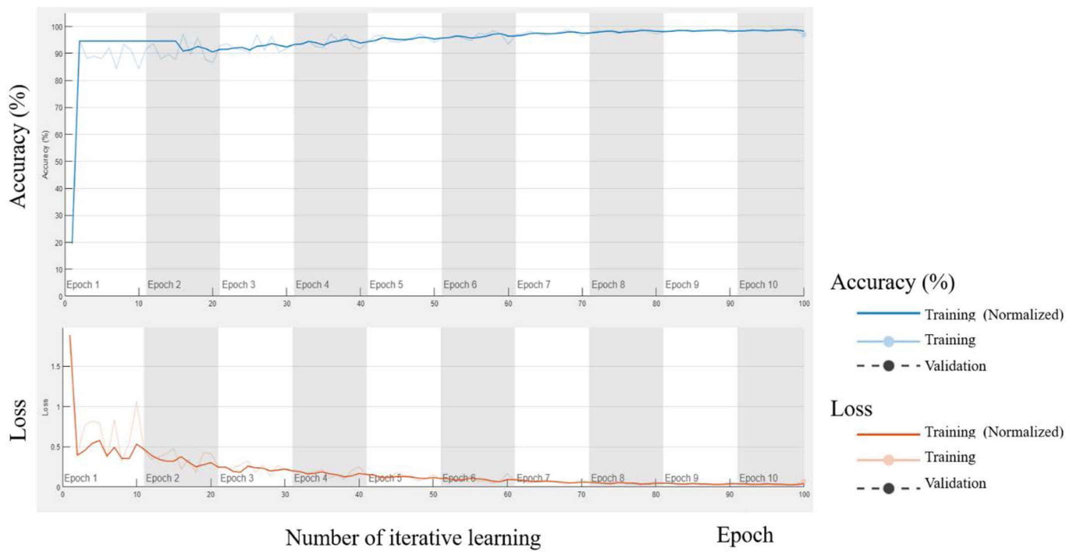

Fig. 4. (Color online) Training progress of self-validation (100 % training data). The upper image showed the accuracy graph for 10 epochs. The lower image showed the loss graph for 10 epochs.

Table 1. Classification results with the computational environment (self-training).

Accuracy (%)	Tanning				Mini-batch		Hardware	
	Elapsed Time (sec)	Epoch	Iteration per Epoch	Maximum Iteration	Accuracy	Loss	Learning Rate Schedule	Learning Rate
98.47 %	110	10	10	100	98.47 %	0.0378	Constant	0.01

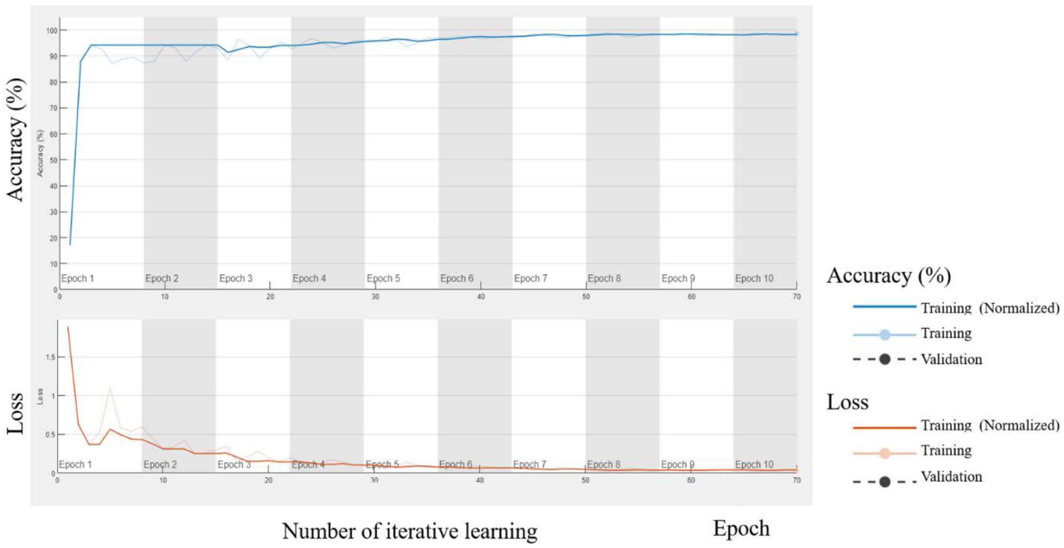

Fig. 5. (Color online) Training progress of cross-validation (70 % training data and 30 % testing data). The upper image showed the accuracy graph for 10 epochs. The lower image showed the loss graph for 10 epochs.

Table 2. Classification results with the computational environment (cross-validation).

Accuracy (%)	Tanning				Mini-batch		Hardware	
	Elapsed Time (sec)	Epoch	Iteration per Epoch	Maximum Iteration	Accuracy	Loss	Learning Rate Schedule	Learning Rate
98.55 %	97	10	7	70	98.55 %	0.0380	Constant	0.01

and Table 2).

3.2. The semantic segmentation mapping

Figure 6 shows the semantic segmentation maps and their ground truth. The ground truth images are manually labeled by human dentistry for validation purposes. AI-segmented maps -Model 1 shows the segmentation map resulted from model 1. Model 1 activated and segmented the same location of ground truth for apical, perio, caries, impaction. However, model 1 had no activation for the abrasion category (Fig. 4, 2nd row, 2nd column). Similarly, AI-segmented maps -Model 2 shows the segmentation map resulted from model 2. Model 2 activated and segmented the same location of ground truth for apical, perio, caries, impaction. However, model 2 had no activation for the abrasion category (Fig. 4, 2nd row, 3rd column). For both models, the activations for apical and perio showed a morphological-close response than caries and impaction categories. And the perio category showed relatively cut-downed mapping size than apical, impaction, caries category.

3.3. Confusion Matrix

Figure 7 shows the confusion matrix of model 1 (a, b) and 2 (c, d). Each confusion matrix refers to the actual class group and predicted class group. The actual class group means the sum sample (pixel) number of each class(category) based on the ground truth images. The predicted class group means the sum sample (pixel) number of each class based on the semantic segmentation maps. The accuracy values (b, d) were driven with the ratio of true positive/all samples (eq. 1). The model 1 resulted 97 %, 91 %, 85 %, 88 %, 0 %, 98 % for 6 category; perio, apical, caries, impaction, abrasion, sounds, respec-

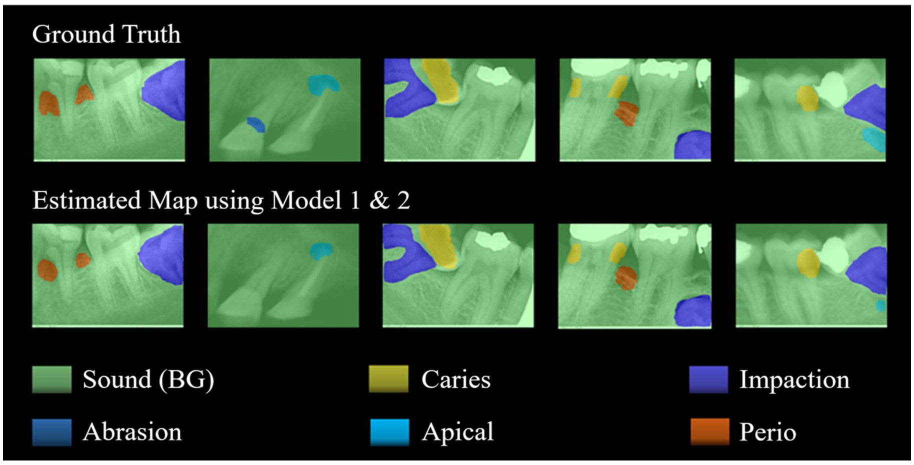

Fig. 6. (Color online) Validation purpose ground truth and semantic segmentation map of the model 1 and 2. The Sound (BG) means normal tissue. Each color means different dental diseases.

Actual class group / Predicted class group

	Perio	Apical	Caries	Impaction	Abrasion	Sound
Perio	**163695**	0	0	10	0	4388
Apical	0	**176050**	0	0	0	17817
Caries	3	0	**435385**	2450	0	71815
Impaction	100	13	14331	**1755387**	0	222316
Abrasion	0	0	0	0	0	0
Sound	134017	101767	134219	149634	16690	**29535849**

(a) Confusion Matrix

Predicted class group — Training (100%)

	Perio	Apical	Caries	Impaction	Abrasion	Sound
Perio	**97%**	0%	0%	0%	0%	3%
Apical	0%	**91%**	0%	0%	0%	9%
Caries	0%	0%	**85%**	0%	0%	14%
Impaction	0%	0%	1%	**88%**	0%	11%
Abrasion	0%	0%	0%	0%	0%	0%
Sound	0%	0%	0%	0%	0%	**98%**

(b) Accuracy

Actual class group

.	Perio	Apical	Caries	Impaction	Abrasion	Sound
Perio	**2289**	0	325	0	0	9256
Apical	0	0	0	0	0	0
Caries	0	0	**4022**	0	0	16540
Impaction	0	0	17481	**308398**	0	106579
Abrasion	0	0	0	0	0	0
Sound	76149	41346	172716	454513	4494	**8743268**

(c) Confusion Matrix

Training (70%) & Test (30%)

	Perio	Apical	Caries	Impaction	Abrasion	Sound
Perio	**19%**	0%	3%	0%	0%	78%
Apical	0%	0%	0%	0%	0%	0%
Caries	0%	0%	**20%**	0%	0%	80%
Impaction	0%	0%	4%	**71%**	0%	25%
Abrasion	0%	0%	0%	0%	0%	0%
Sound	1%	0%	2%	5%	0%	**92%**

(d) Accuracy

Fig. 7. (Color online) Training progress of cross-validation (70 % training data and 30 % testing data).

tively. The model 2 resulted 19 %, 0 %, 20 %, 71 %, 0 %, 92 % for 6 category; perio, apical, caries, impaction, abrasion, sounds, respectively. Model 2 (a, b) had no activation for abrasion. Model 2 (c, d) had no activation for apical and abrasion categories.

3.4. Pros and Cons

The AI study for dental care was conducted to develop a tool that can be helpful for diagnosis in dentistry based on a selected deep learning model. For this, the 86 shared dental x-ray images (from Kaggle) were employed, and then the regions with each dental disease were manually labeled by Oral and Maxillofacial Radiology professional Specialists. Although the dental data used in this study is a very limited amount of 86 images, the possibility of conducting large-scale data-based research can be estimated, and useful information that can reduce trial and error in the future is inferred from the results.

Semantic Segmentation employed in this study can be used to segment a specific area by analyzing image based on the pixel. In particular, Deeplab v3+ which combines Depthwise Separable Convolution and Atrous Convolution has a structure that enables detailed image analysis with less computational load [19]. In this study, Deeplab v3+ showed a very short training time (see Table 1 and 2). Figures 1 and 2 showed the powerful efficiency of Deeplab v3+ for dental radiograph analysis. The classification accuracy was around 98 % although there was a very limited amount of dental images (only 86 images with 5 types). It means that the AI algorithm with a huge data-set will make a promising tool as a clinical application in dentistry. There was a limitation also in Figs. 5 and 6. After full data training (model 2), Abrasion could not be detected by AI since there were only two images that can be training and testing.

In Figs. 4 and 5, the accuracy quickly approaches 99 % in the graph, and the loss curve also quickly reaches a value near 0. Although a limited amount of images were used, the results in Figs. 4 and 5 depicted that the AI model was pretty appropriate to distinguish dental disease lesions. In addition, Fig. 6 shows the ground truth and the regions (model 1 and model 2) estimated by the AI model. First of all, it was confirmed that Model 1 and Model 2 estimated fairly similar patterns, but Abrasion was somewhat difficult to estimate. This is inferred to be since there were a total of two Abrasion samples, which did not provide sufficient amounts for learning and testing.

In Fig. 7, Both models 1 and 2 had no activation for the abrasion category. It is considered due to the limited data amount as mentioned above. Similarly, model 2 had no activation for apical also. The proposed method has limitations by using very limited data numbers to classify the 5 dental diseases. Also, object detection to identify individual teeth. It is necessary to be widely used as a clinical application. As a good clinical application, all processes should be automated on the program.

As a follow-up study, we plan to collect more medical imaging data (more than 10,000). Based on this dental radiography big-data, an additional object detection algorithm will be developed. it will enable the proposed algorithm to automate the entire diagnosis process and is expected to be a technology that can be practically used in clinical practice. We believe that the apical is the most challenging category for semantic segmentation by image feature extraction since the feature of the apical category has similarities with sounds (back-ground feature).

4. Conclusion

In this study, Deeplab_v3 based AI model was employed to demonstrate a possibility for classification of 5 types (perio, caries, apical, impaction, abrasion) of dental diseases using a limited amount of dental X-ray radiographic images. As a result of this study, the AI model showed successful results with the semantic segmentation map image. The semantic segmentation image including diseases image can provide not only objective evidence for the patient but also medical guiding information to diagnose illnesses more quickly and accurately. Especially, these AI-based computational medical technology will be one of the widely used medical applications for the dental radiography area. We believed that the AI model will be a useful tool for the dentist to identify dental diseases in clinical fields.

Acknowledgment

This work was supported by Dongseo University, “Dongseo Cluster Project” Research Fund of 2020 (DSU-2020004).

References

[1] S. B. Khanagar, A. Al-ehaideb, P. C. Maganur, S. Vishwanathaiah, S. Patil, H. A. Baeshen, S. C. Sarode, and S. Bhandi, J. Dent. Sci. (2020).
[2] V. Rajaraman, 198 (2014).
[3] J. Searle, Searle, J. Minds, Brains, Sci. 28 (1984).
[4] https://www.korea.kr/news/policyNewsView.do?newsId=148828131
[5] http://www.kookje.co.kr/news2011/asp/newsbody.asp?code=0300&key=20170125.33001223
[6] http://m.health.chosun.com/svc/news_view.html?contid=2018011100146
[7] T. K. L. Schleyer, T. P. Thyvalikakath, H. Spallek, M. H. Torres-Urquidy, P. Hernandez, and J. Yuhaniak, J. Am. Med. Informatics Assoc. **13**, 344 (2006).
[8] P. F. Whiting, A. W. S. Rutjes, M. E. Westwood, S. Mallett, J. J. Deeks, J. B. Reitsma, M. M. G. Leeflang, J. A. C. Sterne, and P. M. M. Bossuyt, Ann. Intern. Med. **155**, 529 (2011).
[9] K. L. Devito, F. de Souza Barbosa, and W. N. Felippe Filho, Oral Surgery, Oral Med. Oral Pathol. Oral Radiol. Endodontology **106**, 879 (2008).
[10] X. Xie, L. Wang, and A. Wang, Angle Orthod. **80**, 262 (2010).
[11] M. A. Saghiri, K. Asgar, K. K. Boukani, M. Lotfi, H. Aghili, A. Delvarani, K. Karamifar, A. M. Saghiri, P. Mehrvarzfar, and F. Garcia-Godoy, Int. Endod. J. **45**, 257 (2012).
[12] F. Casalegno, T. Newton, R. Daher, M. Abdelaziz, A. Lodi-Rizzini, F. Schürmann, I. Krejci, and H. Markram, J. Dent. Res. **98**, 1227 (2019).
[13] T. Ekert, J. Krois, L. Meinhold, K. Elhennawy, R. Emara, T. Golla, and F. Schwendicke, J. Endod. **45**, 917 (2019).
[14] M. Hung, M. W. Voss, M. N. Rosales, W. Li, W. Su, J. Xu, J. Bounsanga, B. Ruiz-Negrón, E. Lauren, and F. W. Licari, Gerodontology **36**, 395 (2019).
[15] F. Schwendicke, K. Elhennawy, S. Paris, P. Friebertshäuser, and J. Krois, J. Dent. **92**, 103260 (2020).
[16] M. H. Choi, H. Eo, S. E. Jung, H. Woo, W. K. Jeong, J. Y. Hwang, J. S. Lee, J. Il Choi, E. S. Cho, K. H. Do, and S. H. Kim, J. Korean Soc. Radiol. **80**, 684 (2019).
[17] H. Chul, C. Myong, S. Chan, M. Student, and P. S. Chan, **3**, 15 (2020).
[18] J. H. Lee, S. S. Han, Y. H. Kim, C. Lee, and I. Kim, Oral Surg. Oral Med. Oral Pathol. Oral Radiol. **129**, 635 (2020).
[19] L. C. Chen, Y. Zhu, G. Papandreou, F. Schroff, and H. Adam, Lect. Notes Comput. Sci. (Including Subser. Lect. Notes Artif. Intell. Lect. Notes Bioinformatics) **11211 LNCS**, 833 (2018).